MALAYSIAN JOURNAL OF ANALYTICAL SCIENCES

Journal homepage: https://mjas.analis.com.my/

Research Article

Assessing the influence of drying methods on formic acid hydrolysis-derived cellulose from oil palm biomass

Nurizzatul Jannah Hamdan[1], Ahmad Husaini Mohamed[1, *], Noorfatimah Yahaya[2, *], Nur Sofiah Abu Kassim[1], Nur Alia Atiqah Alias[1], Kavirajaa Pandian Sambasevam[1], Siti Nor Atika Baharin[1], Nur Nadia Dzulkifli[1], and Nur Rahimah Said[1]

[1]School of Chemistry and Environment, Universiti Teknologi MARA, Negeri Sembilan Branch, Kuala Pilah Campus, Pekan Parit Tinggi, 72000 Kuala Pilah, Negeri Sembilan, Malaysia
[2]Department of Toxicology, Advanced Medical and Dental Institute (AMDI), Universiti Sains Malaysia, 13200 Bertam Kepala Batas, Penang, Malaysia

[*]Corresponding to: ahmadhusaini@uitm.edu.my; noorfatimah@usm.my

Received: 21 July 2025; Revised: 17 December 2025; Accepted: 5 January 2026; Published: 28 February 2026

Abstract
The study investigated the impact of two drying methods, namely air-drying (AD) and freeze-drying (FD), on the properties of cellulose derived isolated from formic acid hydrolysis. The cellulose was prepared using 60% (v/v) formic acid hydrolysis from oil palm empty fruit bunch (OPEFB) at a solid-to-liquid ratio of 1:20 (g/mL) and then subjected to the two drying methods. The ultraviolet-visible (UV-Vis) spectroscopy analysis revealed that both cellulose samples exhibited sizes within the visible range of 400 to 800 nm, with the highest percentage transmittance being approximately 98%. In terms of morphological analysis, the cellulose obtained after air-drying exhibited a smooth surface, flaky appearance, and agglomeration due to self-organization organisation and stacking between particles. Conversely, cellulose obtained from freeze-drying displayed a rough surface structure, along with self-organisation and stacking between particles. The formic acid hydrolysis technique yielded cellulose with crystallinity properties of 75.98% when freeze-dried and 65.46% when air-dried, while maintaining cellulose type I structure in both cases. This study provides insights into how the drying process following acid hydrolysis can influence cellulose properties, offering opportunities for tailoring cellulose properties for specific applications.

Keywords: cellulose, oil palm empty fruit bunch, acid hydrolysis, drying method

Introduction

In 2023, the production of Malaysian crude palm oil (CPO) was estimated to beat around 18.6 million tons. In this regard, it would be expected that the production of oil palm biomass would also correlate with the production of CPO throughout the year. Among oil palm biomass, oil palm empty fruit bunch (OPEFB) is one of the major wastes produced as a result of pruning and harvesting fresh fruit bunches (FFB). Research on the cellulosic content has reported that OPEFB contains cellulose, constituting 20-50% of its composition, while hemicellulose contributes approximately 23-36%, and lignin accounts for about 14–30%. Hence, due to the abundance and ready availability of OPEFB, coupled with its high cellulose yield which, transforming this oil palm biomass into eco-friendly cellulose materials, presents an alternative solution is presented for to addressing environmental challenges such as waste management and environmental remediation [1, 2].

Cellulose is a polysaccharide composed of repetitive linear chains of glucose units linked by 1,4-β-glycosidic bonds and contains a high number of hydroxyl (-OH) groups on its surface structure. The arrangement and interaction between these -OH groups cause cellulose chains to pack together (forming a cellulose network) through inter- and intramolecular hydrogen bonding as well as van der Waals forces [3]. Typically, the structure of cellulose remains unaffected by diluted acid or alkali chemical treatment. However, subjecting it to various chemical treatment procedures can result in different degrees of degradation and disintegration of hemicellulose and lignin. In our previous study [1], we had

successfully isolated cellulose from OPEFB through a two-step process entailing pre-treatment and bleaching, and a sodium hydroxide alkalisation process. Based on the study, it was observed that the extended, intricate network of hydrogen bonds among cellulose chains is responsible for the aggregation of cellulose structures. Since the final output of cellulose isolation is in slurry or dilute aqueous forms, the use of drying methods becomes highly desirable. Sinquefield et al. [4], in their review, pointed out that the dewatering and drying process poses the main obstacle into successfully preparing cellulose that meets the requirements of certain applications. Drying cellulose materials sometimes leads to irreversible self-agglomeration due to the formation of hydrogen bonds between particles, making them difficult to individualise after drying and redisperse upon rehydration.

For any cellulose materials isolated from various sources, further manipulation of surface structures depends on the selection of the drying methods. This pertains to the proper dewatering of the sample before proceeding with the drying process, which leads to varying self-assembly behaviours and consequently results in different cellulose morphologies and physical properties [5]. In most reported studies, cellulose isolated from various sources is obtained in a suspension form and tends to readily agglomerate during the drying process due to its strong hydrophilic nature. Therefore, producing cellulose in a stable dried form is more practical, particularly for analytical chemistry applications, where it can subsequently be manipulated as an adsorbent for the treatment of environmental pollutants. The cellulose in dried form enhances structural porosity and surface area, increases the availability of active sites, and facilitates surface modification, enabling it to be tailor-made for potential applications as an adsorbent [6,7]. Systematic comparison of cellulose drying methods is essential to elucidate the mechanisms governing pore preservation and accessibility, particularly through the suppression of hornification, which has a direct impact on adsorption efficiency, sensitivity, and reproducibility in analytical applications. Moreover, understanding the influence of drying strategies supports the development of economically viable and scalable cellulose-based materials, enabling their broader implementation as functional adsorbents and analytical platforms for environmental monitoring.

Currently, several drying methods have been introduced for cellulose suspensions, including air-drying, oven-drying, freeze-drying, spray-drying, and supercritical CO_2 spray drying [8]. Oven-drying provides a straightforward drying method that only requires heat and airflow; however this method will cause structural collapse, which can limit the porosity of the cellulose [9,10]. Other than that, the usage of low temperature in freeze-drying helps maintain cellulose quality, with minimal shrinkage and refined pore orientation [11,12]. However, freeze-drying is time-consuming and the cell walls of plant-based materials may be damaged unless rapid freezing is applied. Spray-drying is less time consuming and can dry the cellulose powder efficiently [13].This drying method can be incorporate with surfactants like xanthan gum which can improve the stability and re-dispersibility of the cellulose powder [14], but high temperature and shear during atomisation can degrade its structure. Supercritical CO_2 spray drying remove water from the material above the critical conditions of the solvent used without disturbing the structure of the cellulose, this resulting in high physicochemical stability of the cellulose. However, this method needs solvent exchange due to the immiscibility of CO_2 with water. Some studies show that CO_2 can be combined with organic solvents like ethanol, methanol, acetone and aliphatic alkanes [15].

In drying cellulose, it's crucial to consider its physical morphology and crystallinity, as the absorption of water can disrupt certain properties and reduce the degree of crystallinity in both the cellulose material and its composite. The selection of these two drying methods was guided by techno-economic considerations. Air-drying represents a low-cost and scalable approach, requiring minimal energy input and no vacuum systems or specialized instrumentation, making it attractive for large-scale cellulose production. In contrast, freeze-drying is commonly employed as a benchmark laboratory technique due to its ability to preserve pore structure and suppress hornification, despite its higher energy consumption. Therefore, the present study investigates the effects of air-drying and freeze-drying on the surface morphology and crystalline characteristics of cellulose isolated from OPEFB via formic acid hydrolysis. Following dewatering by filtration, the cellulose was subjected to air-drying and freeze-drying (lyophilization at −57 °C). The resulting materials were comprehensively characterized using scanning electron microscope (SEM) to examine morphological features and x-ray diffraction (XRD) to assess crystallinity, providing insights into how distinct drying pathways affect the structural integrity and functional potential of cellulose for adsorbent applications isolated using mild chemical approach.

Materials and Methods

Material and chemicals

OPEFB was generously donated by Sime Darby Plantation Sdn. Bhd., Labu, Negeri Sembilan, to be used as the source for isolating cellulose. Sodium hydroxide (NaOH), sodium hypochlorite (NaClO, less than 10% active chlorine), formic acid, and hydrochloric acid were procured from R&M

Chemicals (Malaysia). All chemicals were used as received without further purification.

Isolation of cellulose from OPEFB

As soon as the OPEFB was obtained, the fibres were cut into small pieces and rinsed with an excess amount of water to remove oil and impurities. Subsequently, they were oven-dried at 100°C until all moisture was completely removed. The dried fibres were crushed and passed through a 500 µm aperture sieve to achieve a uniform and fine powder. For the isolation of cellulose materials, a two-step process involving alkali pre-treatment, bleaching, and formic acid hydrolysis was utilised (**Figure 1**), following a method previously reported by Jumhuri et al. [16]. The OPEFB fibres underwent an initial pre-treatment process by continuous stirring with 3% (w/v) NaOH, with a solid to liquid ratio of 1:10 (g/mL), for 3 hours at 100 °C. Subsequently, the treated fibres were rinsed with 1% hydrochloric acid solution until the pH became neutral and then filtered. Following this, the fibres underwent multiple bleaching cycles using sodium hypochlorite at 80 °C for 2 hours per cycle until whitish fibres were obtained. The bleached fibres were neutralised with water, filtered, and oven-dried at 60 °C to a constant weight, and were subsequently used as control sample in this study. The cellulose was isolated using 60% (v/v) formic acid hydrolysis for 90 minutes at 45 °C under strong agitation. The reaction with formic acid was quenched by adding ten times the volume of cold deionised water and then subjecting it to 30 minutes of ultrasonication in an ice water bath to disperse the cellulose. The dispersed cellulose was then filtered, thoroughly washed, and dried using two different methods: air-drying (AD) at ambient temperature (25 °C) and freeze-drying (FD) at -57 °C under a pressure of 40 mTorr. The cellulose samples were labelled according to the drying methods applied. For instance, cellulose dried with air-drying was labelled as AD-cell, and cellulose dried with freeze-drying was labelled as FD-cell.

Characterisation analysis

Cellulose was characterised using several instruments and methods, including UV-Visible spectrometry (UV-Vis), attenuated total reflectance–fourier transform infrared (ATR-FTIR), SEM, and XRD. To evaluate the optical characteristics and discern the light absorption and scattering properties of cellulose, UV-Vis spectrophotometry (T 80+) was employed within the range of 400 to 800 nm. The surface morphology of the two cellulose samples (AD and FD) was characterized using scanning electron microscopy (Jeol JSM-6390, USA). The functional groups of the obtained cellulose were recorded using a Perkin Elmer 100 ATR-FT-IR spectrometer (Massachusetts, USA), ranging from 650 to 4000 cm^{-1} with a resolution of 4 cm^{-1}, and an average of 32 scans at each position. The cellulose spectra were compared with those of raw OPEFB and pre-treated-bleached OPEFB. XRD analysis was conducted using a Bruker D8 ADVANCE X-ray diffractometer (Bruker, Germany) equipped with Ni-filtered Cu Kα radiation. The instrument was operated at 40 kV and 40 mA for voltage and current, respectively. Data were collected within a 2θ angle range of 5 to 80°, with an exposure time of 0.1-0.2 sec per step. The crystallinity index (CI) was calculated according to Segal's method using Eq. 1, where $I_{(200)}$ represents the maximum diffraction intensity of the (200) plane, and $I_{(am)}$ indicates the minimum amorphous diffraction intensity between $I_{(200)}$ and $I_{(110)}$ at 2θ.

$$\text{Crystallinity index (CI)} = \frac{I_{(200)} - I_{(am)}}{I_{(200)}} \times 100 \quad \text{(Eq.1)}$$

Results and Discussion

Cellulose materials were extracted from OPEFB biomass through three critical steps, as illustrated in Error! Reference source not found.. Initially, the OPEFB fibres underwent alkalization using 3% (w/v) NaOH, followed by several bleaching cycles with NaClO, and subsequent hydrolysis using 60% formic acid (organic acid) for 90 minutes. During the hydrolysis process, ultrasonication was employed to accelerate the individualisation and dispersion of cellulose particles in cold water suspension. Formic acid was selected as the organic acid in this study due to its stability in dissolving and interacting with non-cellulosic components, such as hemicelluloses and lignin, in an aqueous medium, which is the primary factor contributing to the extraction yield of 65.30%. This yield was comparable to the previously reported yield of 65.78% by Yimlamai et al. [17], who isolated OPEFB using a two-step peracetic acid and alkaline peroxide treatment for 120 minutes. **Figure 2** depicts the UV-Vis spectrum for the optical transparency analysis of isolated cellulose from the OPEFB. The pattern indicates that at lower wavelengths below 500 nm, cellulose particles appear to block light within this region, possibly due to agglomeration. This phenomenon occurs because UV-Vis transmittance is wavelength-dependent, and when light reaches the diameter of the particles [18,19]. Transmittance reaches nearly 100% at wavelengths between 510 to 800 nm, suggesting that the average particle size is less than 800 nm.

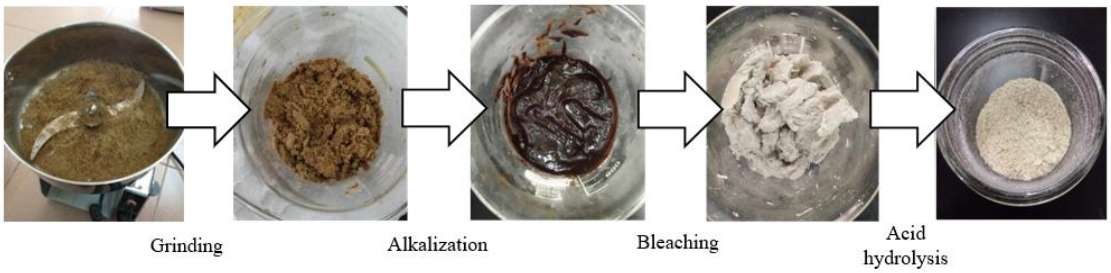

Figure. 1 Acid hydrolysis using 60% formic acid

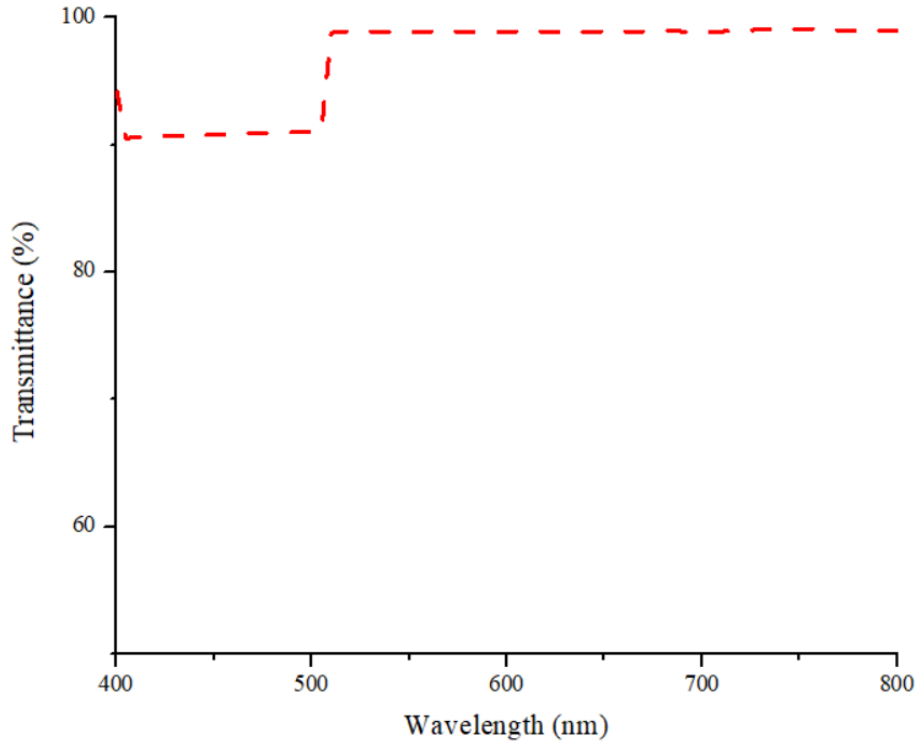

Figure 2. The visible light transmittance spectra of cellulose after formic acid hydrolysis.

Figure 3a-d displays the SEM images of the surface morphologies of raw OPEFB, pre-treated-bleached OPEFB, FD-cell, and AD-cell. The images reveal that all materials exhibit irregular fibrous and non-homogeneous surface structures. The raw OPEFB (**Figure 3a**) exhibits a smooth outer surface structure and is compactly packed. This smooth structure is consistent with other findings which reported the presence of various substances such as lignin, oil, and wax [20]. After pre-treatment with NaOH and bleaching using NaClO (**Figure 3b**), the surface structure becomes pitted and grooved, indicating that impurities such as hemicelluloses and lignin constituents have been dissolved [21]. For freeze-dried cellulose (FD-cell) (**Figure 3c**), the material was curbed with ice particles during the freezing process, which increased the interaction between the cellulose particles. At this stage of drying, interactions between the particles increase, leading to the formation of strong and bulky aggregates. Additionally, agglomeration was attributed to the presence of Van der Waals forces, which bind cellulose particles together. Consequently, a rough surface structure was observed, along with self-organization and stacking between particles [22]. As for air-dried cellulose (AD-cell) (**Figure 3d**), the surface structure forms a solid-packed and very smooth top surface. Similar to the FD-cell, during the air-drying process, the evaporation of water took place at a slow rate, allowing the AD-cell to rearrange and create strong hydrogen bonding networks until a constant weight was achieved. This occurs as a result of reduced steric hindrance effects on the neighbouring structure and high surface energy [23].

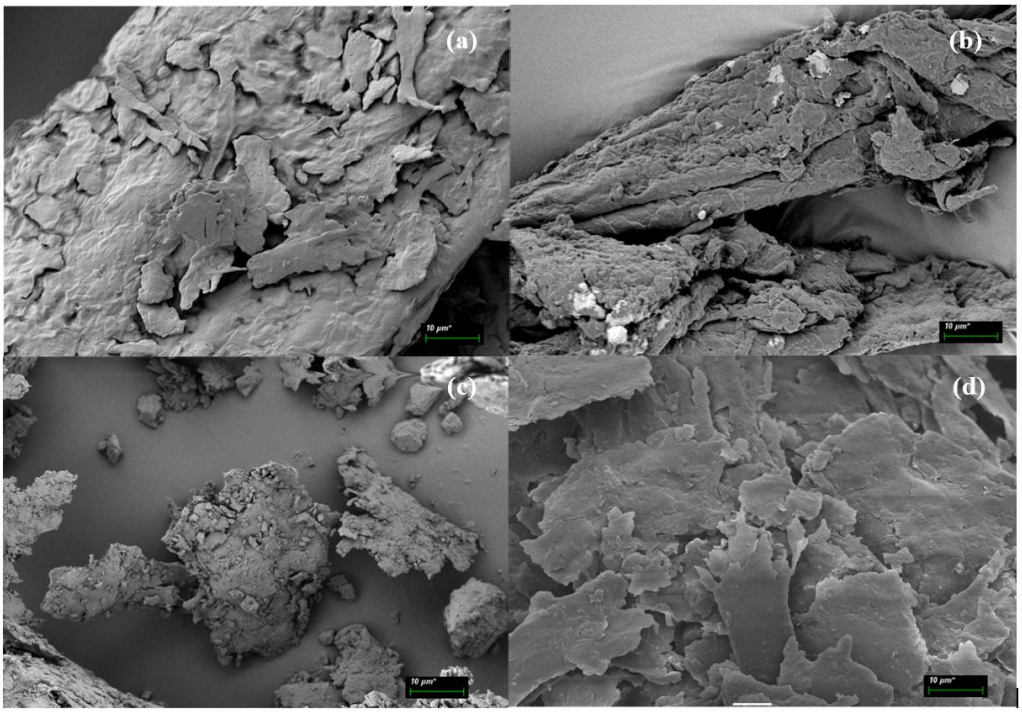

Figure 3. SEM images for the (a) raw OPEFB, (b) pre-treated-bleached OPEFB, (c) FD-cell, and (d) AD-cell at 1,000 magnifications

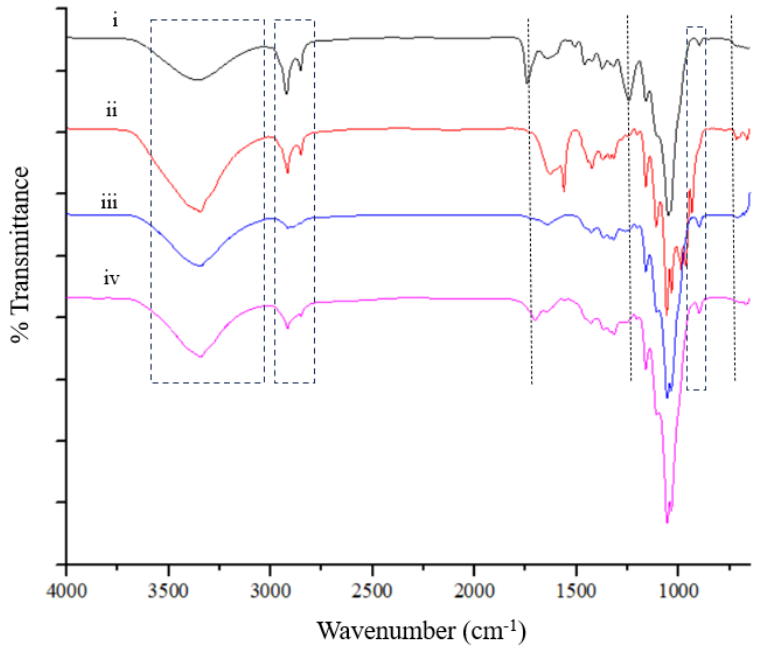

Figure. 4 FTIR spectra of OPEFB fibre after formic acid hydrolysis treatment. The spectra from (i) to (iv) corresponds to the sample (i) raw OPEFB, (ii) pre-treated-bleached OPEFB (iii) AD-cell; and (iv) FD-cell.

The FTIR spectra of formic acid hydrolysis of OPEFB fibre are shown in **Figure 4i-iv.** The bands of -OH and aliphatic saturated -CH_2 stretching, observed between 3300-3700 cm^{-1} and 2800-3050 cm^{-1}, respectively, are distinguished characteristics of the cellulose structure. After pre-treating and bleaching the OPEFB (**Figure 4ii**) with 3% (w/v) NaOH and NaClO (repeatedly), intense bands at 1237 cm^{-1} and 1738 cm^{-1}, which correspond to acetyl and uronic ester groups of hemicelluloses or the ester linkage of the carboxylic group of ferulic and p-coumaric acids in lignin and/or hemicelluloses, were found to have completely disappeared. This indicates the successful removal of hemicellulose and lignin

substituents from the OPEFB fibres [1]. The absorption band between 1645 cm^{-1} and 1695 cm^{-1} is associated with water absorbed within the cellulose structure. This occurs due to the bending modes of water molecules, forming strong interactions with cellulose structures. In addition, bands around 900 cm^{-1} were found in all spectra, signalling C-H rocking vibrations of cellulose specific for C_1–O–C (β-(1–4)-glycosidic linkages [24]. The peak at 717 cm^{-1}, attributed to cellulose 1β in the pre-treated-bleached OPEFB (**Figure 4ii**), disappeared after acid hydrolysis (**Figure 4iii-iv**) suggesting that the cellulose structure was composed solely of the one-chain triclinic structure, Iα (or cellulose 1α) [25]. Finally, absorption bands at 1055 cm^{-1} and 1164 cm^{-1} correspond to the C–O–C pyranose ring stretching vibration in the cellulose structure. This strongly confirms that there were no structural changes after acid hydrolysis of the fibre.

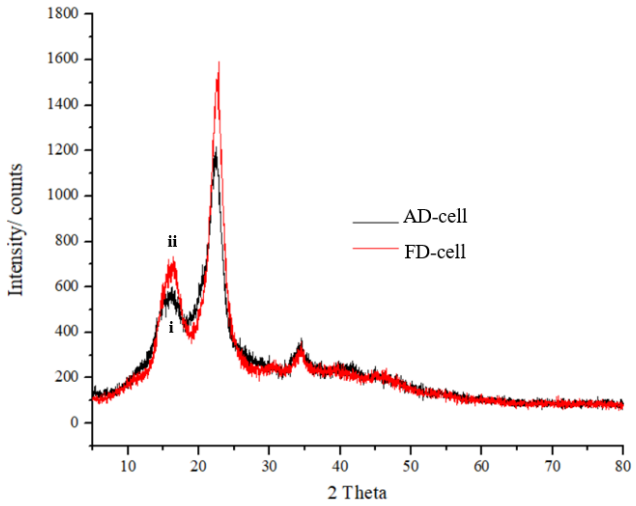

Figure. 5 X-ray Diffraction (XRD) spectra of cellulose with different drying methods i) air-drying (AD-cell), and ii) freeze-drying (FD-cell)

Crystallinity analysis is an important structural assessment for adsorbent materials because it directly influences surface accessibility, chemical stability, mechanical strength, and adsorption behaviour. The XRD spectra of dried cellulose (AD-cell and FD-cell) are shown in **Figure. 5**. The diffraction patterns revealed peaks representing various crystalline planes. Three prominent peaks were observed at 2θ = 16.3°, 22.6°, and 34.6° with Miller indices of (110), (200), and (004), respectively. These peaks signify crystal polymorphs characteristic of cellulose type 1, with no presence of cellulose II (as evidenced by the absence of the doublet at 22.6°), which is commonly found in native plant cellulose, including oil palm. The crystallinity index (CI) of the AD-cell and FD-cell, determined using Segal's method, are 65.46% and 75.98%, respectively [16]. The higher crystallinity index (CI) in FD-cell compared to AD-cell can be attributed to the rearrangement of cellulose fibres. This rearrangement is driven by hydrogen bonding, causing the cellulose to approach each other and form strong aggregates, resulting in the formation of crystalline regions. Notably, the crystalline regions remained unchanged throughout the drying process [23].

Conclusion

Cellulose was isolated from OPEFB using formic acid hydrolysis and then subjected to two different drying methods: air-drying and freeze-drying. Each drying method produced similar functional groups but different morphologies and crystallinity properties. Based on the surface morphology analysis, distinct differences were observed between the AD-cell and FD-cell samples. The FD-cell exhibited enhanced particle–particle interactions, resulting in the formation of strong and bulky aggregates. This behaviour is attributed to intensify van der Waals forces and self-organization processes, which collectively produced a rough and heterogeneous surface structure. In contrast, the AD-cell displayed a much smoother surface morphology, likely due to the rearrangement of neighbouring particles through extensive hydrogen-bonding networks. These interactions reduce steric hindrance and promote a more uniform and compact surface arrangement. Although FTIR analysis confirmed that both materials retained similar functional groups and preserved the characteristic cellulose I structure, XRD results demonstrated that FD-cell exhibited significantly higher crystallinity than AD-cell. This enhancement is attributed to more effective hydrogen-bond rearrangement during freeze-drying, which promotes stronger intermolecular aggregation and a higher degree of structural ordering. To sum, these findings identify freeze drying as a superior approach for maintaining the microstructural integrity and crystallinity of formic acid derived

cellulose, while air drying provide more simpler and more economical results in reduced structural ordering and flattened surface structure. Together, these analyses elucidate how drying methods influence the availability of active sites, pore accessibility, and ultimately the adsorption performance of the material for future adsorbent development.

Acknowledgement

This work was supported by the Malaysian Ministry of Higher Education through the Fundamental Research Grant Scheme (FRGS) [Grant number: FRGS/1/2023/STG04/UITM/03/1] and Geran Insentif Penyelidikan [Grant number: 600-RMC/GIP 5/3 (072/2023)].

References

1. Mohamed, A. H., et al. (2022). Synthesis of oil palm empty fruit bunch-based magnetic-carboxymethyl cellulose nanofiber composite for magnetic solid-phase extraction of organophosphorus pesticides in environmental water samples. *Microchemical Journal,* 183, 108045.
2. Daneshfozoun, S., Abdullah, M. A., & Abdullah, B. (2017). Preparation and characterization of magnetic biosorbent based on oil palm empty fruit bunch fibers, cellulose and *Ceiba pentandra* for heavy metal ions removal. *Industrial Crops and Products,* 105, 93–103.
3. Azani, N. F. S. M., Haafiz, M. K. M., Zahari, A., Poinsignon, S., Brosse, N., & Hussin, M. H. (2020). Preparation and characterizations of oil palm fronds cellulose nanocrystal (OPF-CNC) as reinforcing filler in epoxy-Zn rich coating for mild steel corrosion protection. *International Journal of Biological Macromolecules,* 153, 385–398.
4. Sinquefield, S., Ciesielski, P. N., Li, K., Gardner, D. J., & Ozcan, S. (2020). Nanocellulose dewatering and drying: Current state and future perspectives. *ACS Sustainable Chemistry & Engineering, 8*(26), 9601–9615.
5. Wang, Q., Yao, Q., Liu, J., Sun, J., Zhu, Q., & Chen, H. (2019). Processing nanocellulose to bulk materials: A review. *Cellulose,* 26(13–14), 7585–7617.
6. Darmenbayeva, A., et al. (2024). Cellulose-based sorbents: A comprehensive review of current advances in water remediation and future prospects. *Molecules, 29*(24), 5969.
7. El Mahdaoui, A., Radi, S., Elidrissi, A., Faustino, M. A. F., Neves, M. G. P. M. S., & Moura, N. M. M. (2024). Progress in the modification of cellulose-based adsorbents for the removal of toxic heavy metal ions. *Journal of Environmental Chemical Engineering*, 2024, 113870.
8. Kutová, A., et al. (2021). Influence of drying method and argon plasma modification of bacterial nanocellulose on keratinocyte adhesion and growth. *Nanomaterials,* 11(8), 1916.
9. Wang, L., Tian, Y., Chang, Y., Chen, L., & Zhang, Q. (2025). Cellulose nanofiber-created air barrier enabling closed-cell foams prepared via oven-drying. *Carbohydrate Polymers, 351*, 123096.
10. Schiele, C., et al. (2024). The influence of drying routes on the properties of anisotropic all-cellulose composite foams from post-consumer cotton clothing. *Nanoscale, 16*(30), 14275–14286.
11. Ruan, J.-Q., et al. (2024). Effects of freeze-drying processes on the acoustic absorption performance of sustainable cellulose nanocrystal aerogels. *Gels,* 10(2), 141.
12. Bhatta, S., Janezic, T. S., & Ratti, C. (2020). Freeze-drying of plant-based foods. *Foods, 9*(1), 87.
13. Amin, M. C. I. M., Abadi, A. G., & Katas, H. (2014). Purification, characterization and comparative studies of spray-dried bacterial cellulose microparticles. *Carbohydrate Polymers,* 99, 180–189.
14. Sungsinchai, S., Niamnuy, C., Wattanapan, P., Charoenchaitrakool, M., & Devahastin, S. (2022). Spray drying of non-chemically prepared nanofibrillated cellulose: Improving water redispersibility of the dried product. *International Journal of Biological Macromolecules,* 207, 434–442.
15. Pravallika, K., Chakraborty, S., & Singhal, R. S. (2023). Supercritical drying of food products: An insightful review. *Journal of Food Engineering,* 343, 111375.
16. Jumhuri, A. A., Fatanah, D. N. E., Mohamed, A. H., Hak, C. R. C., Sapari, J. M., & Dzulkifli, N. N. (2017). Characterization of cellulose nanocrystal isolated from oil palm empty fruit bunch using formic acid hydrolysis. *International Journal of Agriculture,* 5, 52–59.
17. Yimlamai, B., Choorit, W., Chisti, Y., & Prasertsan, P. (2021). Cellulose from oil palm empty fruit bunch fiber and its conversion to carboxymethylcellulose. *Journal of Chemical Technology & Biotechnology,* 96(6), 1656–1666.
18. Ching, Y. C., & Ng, T. S. (2014). Effect of preparation conditions on cellulose from oil palm empty fruit bunch fiber. *BioResources, 9*(4), 6373–6385.
19. Saito, T., Nishiyama, Y., Putaux, J.-L., Vignon, M., & Isogai, A. (2006). Homogeneous suspensions of individualized microfibrils from TEMPO-catalyzed oxidation of native cellulose. *Biomacromolecules, 7*(6), 1687–1691.

20. Chiang, A. K. M., et al. (2023). Conversion of palm oil empty fruit bunches to highly stable and fluorescent graphene oxide quantum dots: An eco-friendly approach. *Materials Chemistry and Physics,* 309, 128433.
21. Loke, A. T. T., Dzulkafly, N. S., & Rashid, A. A. (2022). Oil palm empty fruit bunch cellulose fillers as alternative fillers for carboxylated nitrile butadiene rubber latex films. *Materials Today: Proceedings,* 66, 3092–3096.
22. Maria, W. E., Kusumawati, E., Regiana, A., & Suminar, D. R. (2020). Production nanocellulose from raw materials for oil palm empty bunches (TKKS) with hydrolysis and freeze drying methods. *IOP Conference Series: Materials Science and Engineering,* 742(1), 012033.
23. Peng, Y., Gardner, D. J., Han, Y., Kiziltas, A., Cai, Z., & Tshabalala, M. A. (2013). Influence of drying method on the material properties of nanocellulose I: Thermostability and crystallinity. *Cellulose,* 20(5), 2379–2392.
24. Mohamad Haafiz, M. K., Eichhorn, S. J., Hassan, A., and Jawaid, M. (2013). Isolation and characterization of microcrystalline cellulose from oil palm biomass residue. *Carbohydrate Polymers,* 93(2), 628–634.
25. Oun, A. A., & Rhim, J. W. (2015). Effect of post-treatments and concentration of cotton linter cellulose nanocrystals on the properties of agar-based nanocomposite films. *Carbohydrate Polymers,* 134, 20–29.